*Journal of Thermal Analysis, Vol. 38 (1992) 181-196*

# NEW DEVELOPMENTS IN THE FIELD OF PIEZOTHERMAL ANALYSIS

## An experimental approach to the solid state transitions in the case of n–alkanes $C_{21}$, $C_{23}$ and $C_{25}$

*L. Ter Minassian and F. Milliou*

LABORATOIRE DE CHIMIE PHYSIQUE, 11 RUE P. ET M. CURIE 75231 PARIS, CEDEX 05, FRANCE

The solid transitions of $C_{21}$, $C_{23}$ and $C_{25}$ *n*-paraffins are examined from a piezothermal point of view. The paper is divided into two parts. The first is a report of the main features of a piezothermal analyzer when pressure scanning allows the continuous record of the expansivity as a function of pressure up to 5 Kilobars. Small samples are required and the scanning speeds vary from 0.3 to 16 Kilobars per hour. The second part describes the experimental procedure appropriate for solid state determinations. The resulting piezothermograms are presented and entropies of transformation are determined. A model allows a crude statistical approach giving the entropies of transformation with the correct order of magnitude. Problems related with phase transformations under a shearing stress are considered.

**Keywords:** piezothermal analysis, solid state transitions

### Part I

Heat is liberated when a hydrostatic constraint is applied on matter. The exact formulation of the experiment in terms of thermodynamic variables have been achieved since the 19th century and inspired us a new method for the determination of the expansivity of matter by measuring its heat of compression. The method is based on the thermodynamic equation of Maxwell [1], which gives the isothermal variation of the entropy $S$, resulting from a variation of the pressure $p$:

$$\left(\frac{\partial S}{\partial p}\right)_T = -\left(\frac{\partial V}{\partial T}\right)_p \tag{1}$$

*John Wiley & Sons, Limited, Chichester*
*Akadémiai Kiadó, Budapest*

or

$$\delta q_m = -T \cdot \left(\frac{\partial V}{\partial T}\right)_p \mathrm{d}p \tag{2}$$

where $\delta q_m$ is the quantity of heat liberated by one mole.

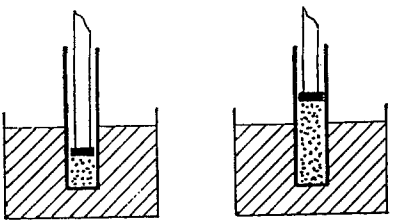


**Fig. 1** Determination of the quantity of heat liberated from: a) constant mass, b) A constant volume

According to the experimental arrangement, the quantity of heat may refer to a constant quantity of matter or originate from a constant volume (Figs 1a, b). We have respectively:

$$\delta q_o = -\alpha_o T v_o \, \mathrm{d}p, \quad \alpha_o = \frac{1}{V_o} \cdot \left(\frac{\partial V}{\partial T}\right)_p \tag{3}$$

where $v_o$ and $V_o$ are the volume of the sample and the molar volume in their initial conditions respectively, or:

$$\delta q_e = -\alpha T v_e \, \mathrm{d}p, \quad \alpha = \frac{1}{V} \cdot \left(\frac{\partial V}{\partial T}\right)_p \tag{4}$$

where $v_e$ is the volume of the vessel.

Equations 3 and 4, originate the piezothermal method for the determination of the quantities $\alpha$ or $\alpha_o$, by an association of the techniques of calorimetry with the high pressure ones.

The conventional devices of our laboratory, mainly consist of an autoclave introduced into the cell of an isothermal calorimeter such as the fluxmeter or the pneumatic calorimeter [2]. Another type of device should be mentioned where the autoclave itself is one of the elements of a twin calorimeter [3, 4]. They allow the direct determination of $\alpha$ or $\alpha_o$ with a pressure independent accuracy of $10^{-2}$ without any special technical improvement. The devices are of a hand driven type and the procedure con-

sists of performing small pressure steps and determine the corresponding quantity of heat liberated at the end of each step. Operating by decreasing or increasing pressures, various type of thermodynamic behaviour have been observed up to 5 or 7 kilobars such as the equation of state of the pure liquids [5–7], liquid mixtures and their demixion [8], phase transitions in the solid [9] or the liquid state [9, 10].

**The piezothermal analyzer (PTA)**

The PTA is an automated device allowing the determination of the $\alpha$ quantities as a function of pressure. It was designed for a twofold purpose: The first was to reduce the quantity of sample from an order of magnitude (1000 down to 100 $mm^3$) for sophisticated chemical preparations. The second one – trivial but important – was to reduce the duration of the measurements which is of an order of six to ten hours for a single isotherm. This duration is a consequence of the step by step method which can be replaced by a continuous one when the derivative of Eq. 4 as a function of time, is considered:

$$J = \frac{\delta q_e}{dt} = -\alpha T v_e \cdot \frac{dp}{dt} \quad (J = \text{heat flux}) \tag{5}$$

Achieving a constant variation of the pressure of slope $B$, we have:

$$J = -\alpha T v_e B, \quad B = \text{constant} \tag{6}$$

A diagram of the analyzer is given in Fig. 2. The flux $J$ is detected with a set of thermocouples tightened between two parallel elements. One of them is a high pressure capillary tube ($\Phi_i = 0.5$ mm, $\Phi_e = 3$ mm), while the other is streched resistance wire for calibration purposes. The arrangement is symmetrical and operates according to the thermal scheme given in Fig. 3. Analysis of the thermal fluxes combined with our calibration method are given in the appendix. The result in terms of the e.m.f. of the thermocouples $e$, and of the calibration constant $\Sigma$ is :

$$\Sigma \frac{J}{l} = \tau \cdot \frac{de}{dt} + e \tag{7}$$

where the quantity $l$ is an effective length and $\tau$ is the time constant of the arrangement.

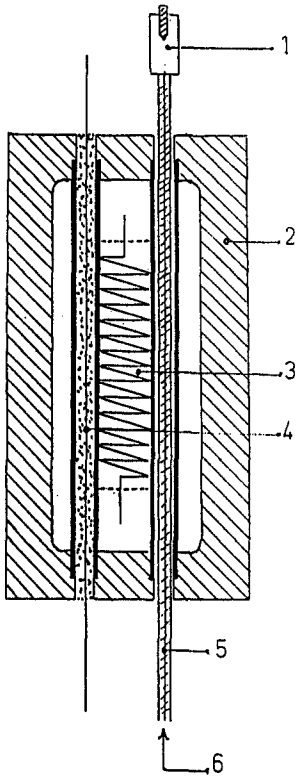


**Fig. 2** The analyzer: 1) H.P. closure 2) containing metal box, 3) the set of thermocouples, 4) resistance wire, 5) H.P. tube, 6) inlet of mercury

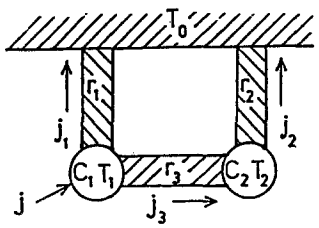


**Fig. 3** The thermal diagram: the difference ($T_1$–$T_2$) is determined from either part of the thermal resistance $r_3 = R$ of the thermocouples. In our case $C_1 = C_2 = C$ and $r_1 = r_2 = r$

Let $s$ be the internal cross sectional area of the high pressure tube. Equations 6 and 7 together with $v_e = sl$, give a formulation where the quantity $l$ has cancelled out:

$$\alpha = \frac{\tau \cdot \frac{de}{dt} + e}{T s B \Sigma} \tag{8}$$

Equation 8 indicates that the thermoelectric signal should be corrected by its time derivative. Finally, as the measured heat of compression is composed of the added contributions of the content and its container, Eq. 8 should be corrected:

$$\alpha - \alpha_{r=} \frac{\tau \cdot \frac{de}{dt} + e}{T s B \Sigma} \tag{9}$$

where $\alpha_r$ is the expansivity of the container material.

The PTA consists of the following elements:

– The analyzer (Fig. 2) with the high pressure tube positioned into one of its elements. The filling requires a volume of sample of the order of 100 $mm^3$, while the useful quantity is 20 $mm^3$. The time constant is about of $\tau = 40$ seconds.

– A heating chamber containing the analyzer.

– A motorized high pressure pump with the appropriate pressure gauges.

– A nanovoltmeter.

– A micro computer managing the operations and recording the $\alpha$ quantities on an interval of time of 45 seconds.

Characteristics and performances are as follows:

| | |
|---|---|
| – Temperature range: | 25 to 280° |
| – Pressure range: | 0.2 to 6 Kilobars |
| – Scanning speed: | 0.3 to 16 Kilobars/hour |
| – Temperature setting time: | 4 hours |
| – Time constant $\tau$: | 40 seconds |
| – Volume of sample: | 100 $mm^3$ |
| – Stability of the thermoelectric signal: | $10^{-8}$ volts |
| – Sensitivity $\Sigma$: | 0.125 volt · cm/watt |
| – Accuracy $\Delta\alpha / \alpha$: | $10^{-2}$ |
| – Hydraulic fluids: | Hydrocarbons, water, mercury |

*Operating procedures and control*

The analyzer is held vertically in its heating chamber. Compression is performed by the mercury level positioned at the bottom of the H.P. tube.

Driving the mercury up and down in a funnel fitted with the upper end of the tube, ensures easily the filling with most liquids at room temperature. The test is performed with liquid hexane, its piezothermal features having been achieved by our conventional method in a large range of temperature

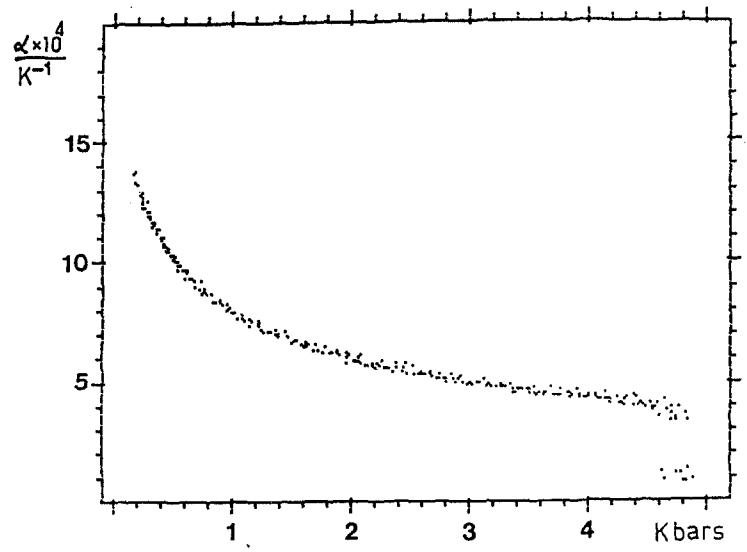


**Fig. 4** Hexane at the temperature of 99.6°C: A superposition of recordings at different scanning speeds. The rates are $B$ =-6, -10, -12 and -16 kilobars/hour

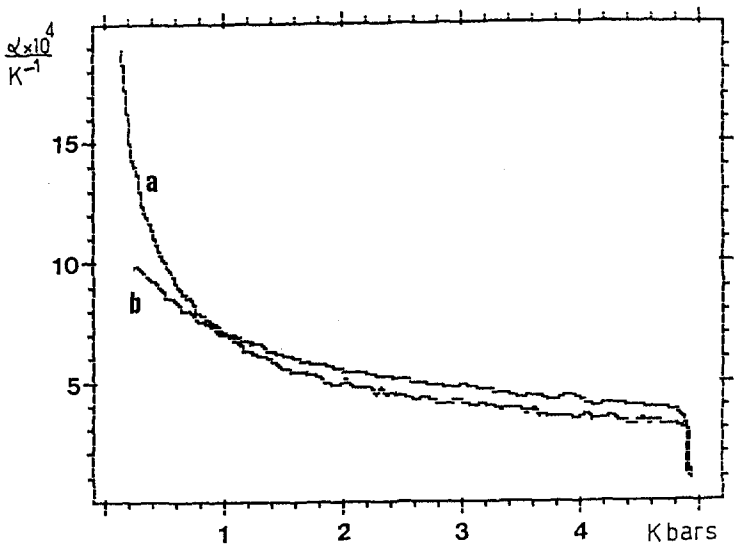


**Fig. 5** Hexane on two isotherms: a) 227.6°C, b) 21.4°C

and pressure. Figure 4 results from a superposition of recordings performed at different speeds in order to check the selected value of $\tau = 40$ seconds. The scatter of the data points may be considered as satisfactory. Figure 5 illustrates the behaviour of the PTA as a function of temperature: two isotherms are shown (26 and 227°), intersecting at a pressure of 900 bars. This is the expected behaviour with the correct pressure. The agreement is also fair when the $\alpha$ curves are compared with the ones resulting from the conventional method [11].

## Part II

Most of the thermodynamic data concerning the *n*-paraffins are collected in the interesting paper of Broadhurst [12], from the $C_2$ up to the $C_{43}$ paraffins showing the existence of two phases before melting. A parity dependent behaviour is observed, such that the paraffins of odd and even numbered carbon atoms fall into two separate categories. The odd numbered ones, in their minimum entropy phase, are characterized by a lamellar structure where the streched chains are perpendicular to the end group planes. The planes of the ribbon like molecules are parallel and rotations about their long axis are restricted. The higher entropy phase would allow their reorientations by jumps of the individual molecules or by a collective mechanism. Let $t_r$ be the transition from one solid phase to the other and $t_f$ the melting transition.

Scanning calorimetry reveals a more complex situation beginning with the $C_{23}$ and $C_{25}$ paraffins, where two additional transitions are detected between $t_r$ and $t_f$ [13, 14]. This result may be compared qualitatively with the one found formerly in the case of the $C_{33}$ paraffin [15], so that one may guess the same general features to be repeated in the case of the chains of intermediate length. It was interesting to approach the same problems by PTA for a quantitative comparison with the DSC determinations. The project required a new experimental procedure appropriate to the solid state.

### *Operating procedure*

The hydraulic fluid of the PTA is mercury and the circuit is connected with a container operating on the principle of the communicating vessels. The device allows the precise adjustment of the levels in the H.P. tube for filling purposes.

– The mercury is positioned on the level of the funnel and the crystals are deposited.

– The heating chamber is set at a significantly higher temperature than the melting point.

– The mercury level is lowered and the system allowed to cool down to room temperature.

When the upper end of the H.P. tube remains opened, our first observation is that mercury percolates across the solid sample when a pressure of 100 bars is applied from the lower end. (The overall length of the H.P. tube is 200 mm). When the upper end is closed and the system is ready for a room temperature determination, the thermoelectric signal triggers beyond a first compression of 100 bars becoming reversible and sensitive under a pressure impulse of a few bars. The same is true up to the highest pressures and also when the first 100 bars range is inspected again.

The explanation is in the existence of mercury streamlets 'irrigating' the sample through the intergranular voids, transmitting the pressure in a direction perpendicular to the axis of the tube. An estimate of the diameter of the streamlets based on a hemispherical meniscus and the observed 100 bars, would lead to a figure of 0.1 micron.

## Results

Most of the determinations are performed by decreasing pressures and at the very low speed of $B = -300$ to $-500$ bars/hour. Figure 6 gives a piezothermal recording in the case of heneicosane ($C_{21}$). The transition $t_r$ is observed on the high pressure side together with the melting transition $t_f$ on the lower side. Two intermediate peaks appear in the case of tricosane ($C_{23}$) on Fig. 7, which we denote by $(t_r + 1)$ and $(t_r + 2)$ respectively in decreasing pressure order. The case of pentacosane ($C_{25}$) is still more complicated with the appearance of an additional transition before melting (Fig. 8). For the sake of discussion, we denote by $(t_f - 1)$ this last transition. The experiment is repeated at the very low speed of $B = -300$ bars/hour giving the piezothermogram (Fig. 9), shown on a different scale. A defect may be observed during the $t_r$ transition and also a remarkable progression in the peak heights by decreasing pressures. Figure 10 illustrates a run performed at a higher temperature: The $t_f$ transition merges with $(t_f - 1)$, whereas $t_r$, $(t_r + 1)$ and $(t_r + 2)$ are unchanged.

The variation of entropy associated with the transition peaks is determined by their area. We note that the measured quantity is $\alpha_o$ rather than $\alpha$,

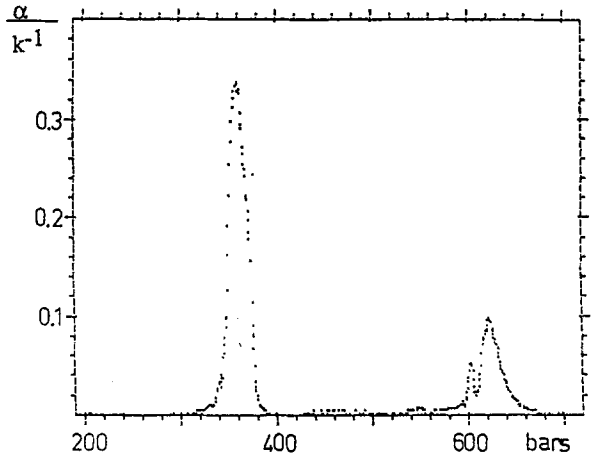


**Fig. 6** Heneicosane at the temperature of 50°C: transition $t_r$ and melting transition $t_f$ on the high and low pressures side respectively

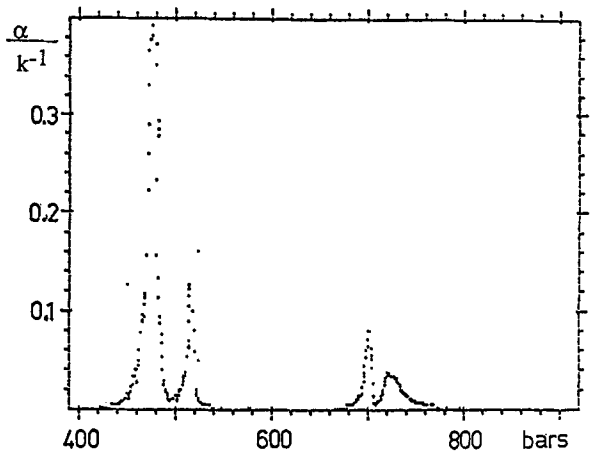


**Fig. 7** Tricosane at the temperature of 59.9°C: by decreasing pressure order ($t_r+1$) and ($t_r+2$) additional transitions are observed

owing to the immobility of the solid phase compressed by mercury. We fall in the case of the Eq. 3 and neglecting the contribution of the mercury, we have:

$$\Delta S = -V_o \int \alpha_o \, dp \tag{10}$$

or

$$\rho_o \cdot \frac{\Delta S}{R} = -\frac{M}{R} \cdot \int \alpha_o \, dp \tag{11}$$

where the entropy is formulated in dimensionless units and where $\rho_o$ is the density in the initial conditions (room temperature and $p = 1$).

The results are given in round figures in Table 1 and show an important dispersal. Joining together the entropy contributions from the $t_r$, $(t_r+1)$ and $(t_r+2)$ transitions reveals figures some 60% higher than those of Broadhurst. The agreement is better in the case of the $t_f$ transitions if we put aside the $(t_f-1)$ transition which occurs in the case of pentacosane. This aspect is a consequence of a too optimistic experimental approach when steep transitions are implied as in the case for melting where our figures show an excess of 20%. In spite of the foregoing limitations, we may compare with DSC

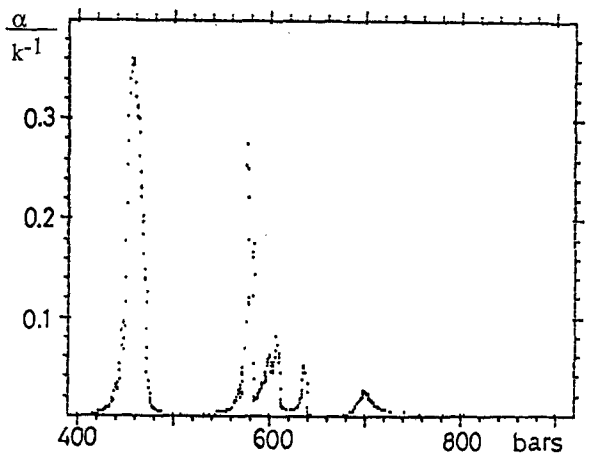


**Fig. 8** Pentacosane at the temperature of 65.1°C: The $(t_f-1)$ appears before melting occurs

**Table 1** Entropy of the $(t)$ transitions in $\rho_o \cdot \Delta S/R$ units (grs·cm$^{-3}$) for different selected runs

| Run $n^o$ | $T$(°C) | $t_r$ | $(t_r+1)$ | $(t_r+2)$ | $(t_f-1)$ | $t_f$ |
|---|---|---|---|---|---|---|
| | | | Heneicosane | | | |
| 1 | 50 | 11 | 0 | 0 | 0 | 26 |
| 3 | 70 | 14 | 0 | 0 | 0 | 25.5 |
| | | | Tricosane | | | |
| 26 | 60 | 4.5 | 4 | 4 | 0 | 24.5 |
| | | | Pentacosane | | | |
| 18 | 65 | 6 | 1 | 3 | 8 | – |
| 10 | 70 | 3.5 | 5.5 | 3.5 | 8 | 25 |
| 9 | 70 | 7.5 | 3.5 | 2 | | 32.5 |

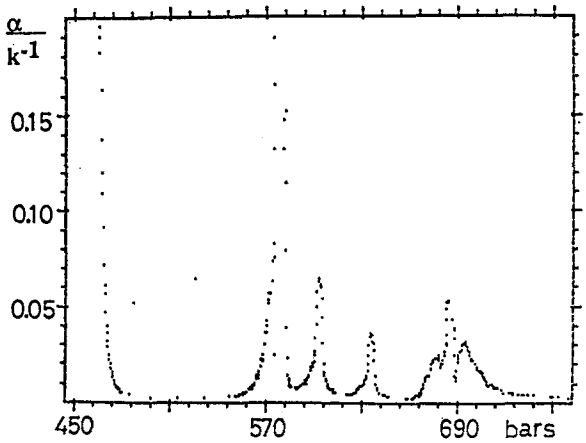


**Fig. 9** Pentacosane at the temperature of 65°C performed at the lowest scanning speed: the same observation as in Fig. 8

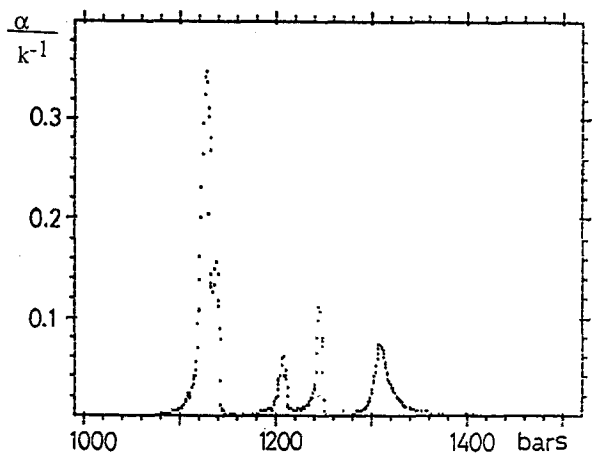


**Fig. 10** Pentacosane at the temperature of 79.8°C: The transition $t_f$ merges with transition ($t_f$–1)

determinations by identifying the $t_r$ transitions in the ascending temperature order. In the case of tricosane the $(t_r+2)$ transition is given with the figures of $\Delta S/R = 0.13$ or 0.04 according to authors [14, 15], whereas the $(t_r+1)$ transition amounts to $\Delta S/R = 0.160$. They are thermodynamically insignificant, a result of which is perhaps the consequence of a poor resolution.

## Discussion

The mechanism of the transitions in the case of *n*-paraffins have been compared to the one which occurs in the case of liquid crystals [16]. The analogy inspires from the lamellar structure where the molecular long axis are perpendicular to the planes of their end groups in the case of odd numbered carbon atoms, or oblique in the case of the even ones. The zigzag structure of the molecule determines a plane along the long axis and in their lowest entropy the molecular planes are parallel. Reorientation occurs with the passage through the $t_r$ transition when the molecular planes may take four or six equivalent positions as have been shown for rigid chains of infinite length [17]. However, the contribution to entropy of the increased statistical weight does not yield the expected value of $\Delta S/R = 4$ to 6.

We consider now a chain of finite length where translation of the molecule along its long axis adds or accompany the reorientations as have been suggested by Stobl [15] in the case of the $C_{33}$ *n*–paraffins. Its effect is to tilt the otherwise parallel molecules, into an oblique angle with the planes of the terminal end groups, the subcell remaining orthorhombic. An alternative has been suggested by Zerbi [18] in the case of the $C_{19}$ *n*–paraffin, the chains are expelled from the lamellar structure, a stem of a few carbon atoms sticking out of the surface. The stems are distorted, trans–gauche positions being allowed in the interlamellar voids, bringing an additional contribution to the number of configurations $W$. A crude approach in terms of the number $n$ of carbon atoms outside of a lamella gives:

$$W = \left[\nu Z^{(n-1)}\right]^N \tag{12}$$

where $\nu$ is the number of equivalent orientations of the plane of the molecule in the lamella and $Z$, the number of directions for each of the C–C bonds in the interlamellar voids. The configurational entropy may be written accordingly:

$$\Delta S/R = (n-1)\cdot \ln Z + \ln \nu \tag{13}$$

Equation 13 would give the transition entropy $t_r$ by an arbitrary, but reasonable, set of the parameters. With $n = 4$, $Z = 3$ and $\nu = 6$, the corresponding figure for entropy is $\Delta S/R = 5.1$. The successive entropy jumps performed by the $(t_r+1)$, $(t_r+2)$ transitions would be estimated by difference:

$$\Delta S/R = \Delta n \cdot \ln Z \tag{14}$$

where $\Delta n$ is the number of additional carbon atoms expelled into the voids.

The final part of our discussion deals with our experimental entropies which are significantly higher than the data given in the literature. Our feeling is that the initial phase we prepare in the PTA at a high pressure and a temperature $T > T_t$, is not the same as the one prepared by the authors at $p = 1$ and $T < T_t$. This difference is a consequence of a non hydrostatic distribution of the constraints introduced by our method of compression. The crystals are compressed against the internal wall of the H.P. tube, bringing a shearing stress with a glide of the lamellas. The otherwise ordered arrangement of the methyl groups, from either part of the interface, should be highly perturbed setting the problem of a new structure for our odd numbered paraffin molecules. In fact, the difference with the even numbered paraffin molecules is entirely governed by steric considerations on the terminal methyl groups. For the odd molecules, the passage to the triclinic high density packing attained by even molecules is considered as impossible inhydrostatic conditions. We think that the restriction has no more to be considered in the case of our strained crystals and that such a transition has occurred during its preparation. With this assumption we compare (Table 2), the overall entropy effects observed in our case with the entropies of the corresponding even molecule having an additional carbon atom. The agreement supports the assumption setting aside however, the case of the $(t_f-1)$ transition observed with our $C_{25}$ molecule. This may be explained by stress recovery interfering in the highly pressure sensitive region of melting.

**Table 2** Entropy of the added contributions of our $t_r$, $(t_r+2)$ transitions (column b) compared with the data of Broadhurst for odd an even $n$-paraffins (column a)

| | (a) | (b) |
|---|---|---|
| C21 | 6.11 | 11 to 14 |
| C22 | 10.3 | – |
| C23 | 8.37 | 12.5 |
| C24 | 11.7 | – |
| C25 | 9.83 | 10 to 13 |
| C26 | 12.7 | – |

## Conclusion

About fifty years ago, Deffet [19] published the first inventory of polymorphic substances with 1200 organic crystals. Nowadays, such a list would contain ten thousands of substances and would illustrate the fragility of any crystalline system with its limited range of stability under the effect of temperature or pressure. The two effects are thermodynamically equivalent but when we approach the solid state, the choice of the two variables ($T$, $p$) is not the most appropriate. In fact, the potential energy mainly governs the behaviour of solids and the volume would be the best variable. From this point of view, the temperature has a twofold action as it modifies together the kinetic energy and the volume while the pressure acts only on the latter. From the experimental point of view, if we consider the volume as the independent variable, the information will be screened if we use the dependent variables $p$ or $T$. However pressure is more effective and direct than temperature. This would explain the better resolution we obtain from pressure scanning when overlapping solid transitions are concerned.

The problem to solve in the future is the quantitive one. Whereas the piezothermal analyzer has proved its adequacy for liquids and gases, it failed to give reliable quantitative results in the case of solid paraffins in their highly pressure sensitive region of melting. It nevertheless allowed us to observe that transitions considered as insignificant from a thermodynamical point of view are, in fact, greater by more than one order of magnitude. Finally, the crystals under shear bring out another problem. The literature on the subject is sparse and essentially related to chemical reactions and it is perhaps the time to approach the problem from a scientific point of view.

## References

1 Maxwell, Theory of heat, Ed. 1871, p. 167.
2 L. Ter Minassian and F. Milliou, J. Phys. E: Sci. Instrum., 16 (1983) 450.
3 P. Pruzan, Université P. et M. Curie, Thèse 1976.
4 L. Ter Minassian P. Pruzan and H. Szwarc, Rev. Sci. Instrum, 47 (1976) 74.
5 L. Ter Minassian and P. Pruzan, J. Chem. Phys. 75 (1981) 3064.
6 C. Alba, L. Ter Minassian, A. Soulard and A. Denis, J. Chem. Phys., 82 (1985) 384.
7 L. Ter Minassian, K. Bouzar and C. Alba, J. Phys. Chem., 92 (1988) 487.
8 L. Ter Minassian and I. Tomaszkiewicz, J. Phys. Chem., 92 (1988) 68.
9 L. Ter Minassian and P. Pruzan, J. Chem. Thermo., 9 (1977) 375.
10 L. Ter Minassian and P. Shashidhar, J. Phys. Lett., 43 (1983) L239.
11 P. Pruzan, J. Phys. Lett., 113 (1984) 4273.
12 M. G. Broadhurst, J. Res. N. B. S. -A Phys. Chem., 66A (1962) 241.
13 J. Doucet, I. Denicolo and A. Craievich, J. Chem. Phys., 75 (1981) 5125.

14 G. Ungar, J. Chem. Phys., 87 (1983) 689.
15 G. Strobl, B. Ewen, E. W. Fisher and W. Piesczek, J. Chem. Phys., 61 (1974) 5257.
16 J. Doucet, I. Denicolo and A. Craievich, J. Chem. Phys., 75 (1981) 1523.
17 T. Yamamoto, J. Chem. Phys., 82 (1985) 3790.; 89 (1988) 2356.
18 G. Zerbi, R. Magni, M. Gussoni, K. H. Moritz, A. Bigotto and S. Dirlikov, J. Chem. Phys., 75 (1981) 3175.
19 L. Deffet, Répertoire des composés organiques polymorphes, Ed. Desoer, Liège 1942.

## Appendix

### *THE THERMAL ASPECTS OF THE DEVICE*

*– Fundamental equations*

$$T_1 - T_0 = r_1 \cdot j_1 \qquad C_1 \, dT_1/dt = J - j_1 - j_3$$

$$T_2 - T_0 = r_2 \cdot j_2$$

$$T_1 - T_2 = r_3 \cdot j_3 \qquad C_2 \, dT_2/dt = j_3 - j_2$$

*– The device is symmetrical*

$r_1 = r_2 = r$, $C_1 = C_2 = C$, and $r_3 = R$

$$\Omega J = \tau \, d\Delta T/dt + \Delta T$$

with

$$\Omega = r \cdot R/(2r + R),$$

$$\tau = \Omega C, \quad \Delta T = T_1 - T_2$$

*– Converting into thermoelectric signal*

$E$ = Thermoelectric power, $e$ = e.m.f.

$$E \, \Omega J = \tau \cdot de/dt + e$$

*– Calibration with the electrical resistance*

$w$ = Heat power released per unit length
$l$ = The effective length of the cell

$$J = w \cdot l$$

*– Determination of the sensitivity $\Sigma$ in the stationary state*

$$\Sigma = e/w = E\,\Omega\,l$$

– *Final formulation*

$$\Sigma J/l = \tau \cdot \mathrm{d}e/\mathrm{d}t + e$$

– The time constant $\tau$ is determined empirically.

**Zusammenfassung** — Feststoffumwandlungen bei $C_{21}$, $C_{23}$ und $C_{25}$ *n*-Paraffinen wurden unter dem Gesichtspunkt der Piezowärme untersucht. Im ersten Teil vorliegender Arbeit werden die Haupteigenschaften eines piezothermischen Analysators beschrieben, bei dem durch Druck-Scanning die kontinuierliche Aufzeichnung des Ausdehnungsvermögens als Funktion des Druckes bis zu 5 kbar ermöglicht wird. Es werden nur kleine Proben benötigt, die Scanning-Geschwindigkeit variiert zwischen 0,3 und 16 kbar/h. Der zweite Teil beschreibt das geeignete experimentelle Verfahren zur Feststoffzustandsbestimmung. Die erhaltenen Piezothermogramme werden dargestellt und die Entropien der Umwandlung bestimmt. Ein Modell liefert eine grobe statistische Näherung, die die Entropien der Umwandlung in der richtigen Größenordnung liefert. Probleme in Zusammenhang mit Phasenumwandlungen bei Scherbeanspruchungen werden betrachtet.